Mineralogical Magazine, August 1999, Vol. 63(4), pp. 447–471

Diamonds from Wellington, NSW: insights into the origin of eastern Australian diamonds

R. M. DAVIES[1], S. Y. O'REILLY[1] AND W. L. GRIFFIN[1,2]

[1] GEMOC National Key Centre, School of Earth Sciences, Macquarie University, Sydney, NSW, 2109, Australia
[2] CSIRO Exploration and Mining, P. O. Box 136, North Ryde, NSW, 1067, Australia

ABSTRACT

Diamonds from alluvial deposits near Wellington, New South Wales, have been characterized on the basis of morphological features, mineral inclusions, C isotope signatures, N content and aggregation state and internal structure. The diamonds are of two types. The larger group (Group A) is indistinguishable from diamonds found worldwide from kimberlitic and lamproitic host rocks. This group is inferred to have formed in a peridotitic mantle source in Pre-Cambrian subcratonic lithosphere. The second group (Group B) is unique in its internal structures (which show evidence of growth in a stress field and non-planar facets), has unusually heavy C isotopic compositions and contains Ca-rich eclogitic inclusions. This group is inferred to have formed in a subducting slab. Diamonds of both groups have external features (corrosion structures and polish) indicating transport to the surface by lamproitic-like magmas. The diamonds show evidence of long residence at the earth's surface and significant alluvial reworking: they are not accompanied by typical diamond indicator minerals.

KEYWORDS: alluvial diamonds, diamond inclusions, carbon isotopes in diamond, diamond deformation, N aggregation in diamond, growth structures in diamond.

Introduction

ECONOMIC concentrations of diamonds occur in kimberlitic and lamproitic intrusions through Archaean and Proterozoic continental crust worldwide and as alluvial deposits derived from these primary sources. Alluvial accumulations of diamonds also occur in areas of Palaeozoic and Mesozoic crust in Burma, Thailand, Kalimantan, the Ural mountains, California and eastern Australia. The primary sources for the eastern Australian alluvial diamond deposits remain unidentified and their origin is obscure: for this reason, they have been referred to as headless placer deposits.

Many headless placer diamond concentrations occur in areas of convergent-margin tectonics (see summary in Griffin *et al.*, 1998), and lack the traditional suite of associated 'indicator minerals'. This situation has led to suggestions that Phanerozoic subduction was involved in the formation and exhumation of the diamonds, without the involvement of conventional kimberlitic or lamproitic volcanism.

Diamonds have been reported in metamorphic rocks from several localities: these include microdiamonds in crustal rocks metamorphosed at high pressures (Kazakhstan: Sobolev and Shatsky (1990); China: Xu *et al.* (1992)); microdiamonds found by processing bulk samples (but not *in situ*) from Norway: Dobrzhinetskaya *et al.* (1995); and microdiamonds from bulk sampling of Tibetan ophiolitic peridotites: Bai *et al.* (1993). The Tibetan diamonds now appear to be synthetic diamonds introduced into the sample during processing (P.H. Nixon, pers. comm.). Graphitized macrodiamond pseudomorphs have been described from pyroxenite layers in large massifs of upper-mantle peridotite exposed in the Betic-Rifean zone of northern Morocco and southern Spain (Pearson *et al.*, 1993, 1995).

Records of diamond discovery in eastern Australian date from 1851 when diamonds were

discovered near Wellington in New South Wales (NSW). In 1872, the largest known accumulations of alluvial diamonds were discovered 600 km to the northeast at Copeton and Bingara, NSW. Total production from these localities to date is approximated at 500,000 carats (Brown, 1995). In contrast to this large concentration of alluvial diamonds, the Wellington region, which includes Airly Mountain, hosts over 100 small alluvial diamond occurrences. Records for production at Wellington and Airly Mountain are ~4,000 and 100 carats respectively (MacNevin, 1977).

Previous work on the eastern Australian diamonds has focused mainly on the Copeton diamonds and include the benchmark study of MacNevin (1977), studies on the Copeton diamonds by Sobolev *et al.* (1984), and by Sobolev (1985) and other studies and discussions documented in papers by O'Reilly (1989), Taylor *et al.* (1990), Sutherland *et al.* (1994), Meyer *et al.* (1995), and recent investigations by Barron *et al.* (1994; 1996), Meyer *et al.* (1997) and Griffin *et al.* (1998).

This study investigates the nature and origin of alluvial diamonds from the Macquarie River near Wellington, NSW, 350 km west of Sydney (Fig. 1) and is part of a wider study of alluvial diamonds from eastern Australia. This is the first comprehensive study of a large number of stones from eastern Australia integrating a broad range of available techniques including morphological studies, cathodoluminescence, N content and aggregation state, C isotopic composition and analysis of inclusions in the diamonds.

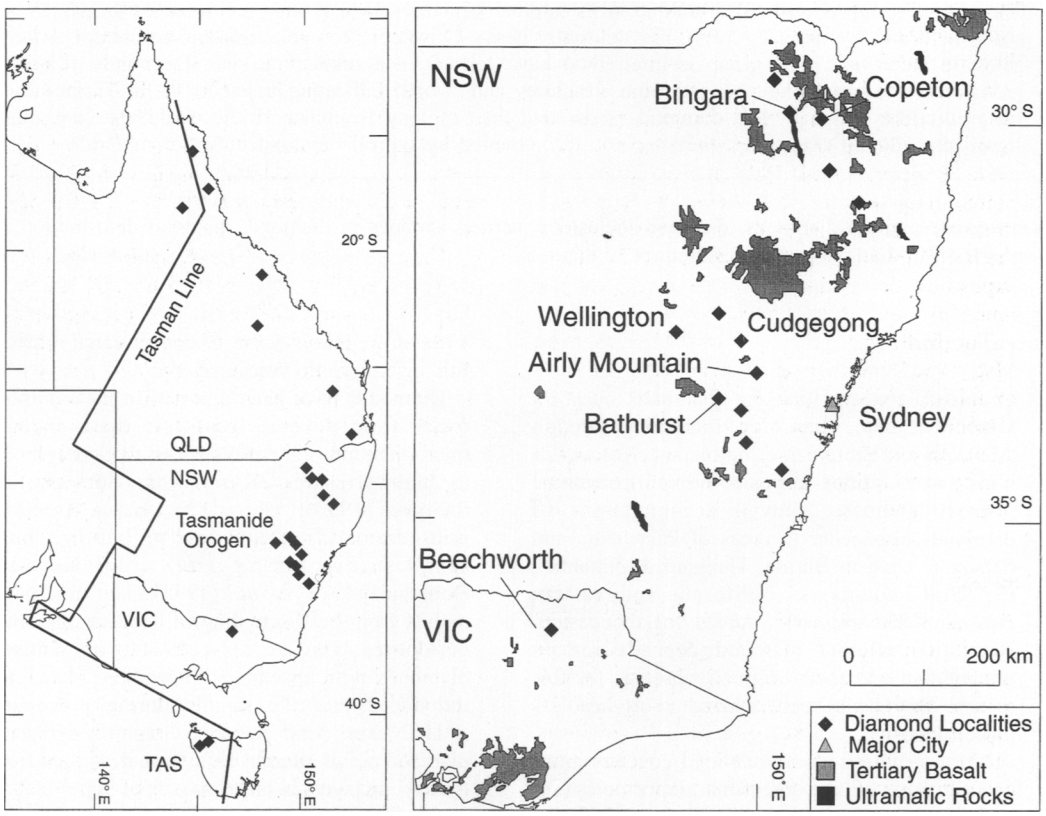

FIG. 1. Distribution of alluvial diamond deposits in eastern Australia, Tertiary basalts and tectonically emplaced Palaeozoic ultramafic rocks in eastern Australia. The Tasman Line represents the boundary of the Palaeozoic Tasmanide Orogen with the western cratonic part of Australia.

Geological setting of eastern Australian diamonds

Diamonds are known from the entire length of the eastern Australian continent, from north Queensland south through New South Wales and Victoria to Tasmania (Fig. 1). They occur in alluvium and in buried alluvium beneath Tertiary basalt flows, show evidence of alluvial reworking, and are not associated with any of the conventional diamond indicator minerals such as chrome spinel, ilmenite, chrome-pyrope garnet and microdiamonds.

Eastern Australia is considered to be a dominantly Phanerozoic terrain, demarcated from the western Proterozoic and Archaean cratonic domains by the Tasman Line (Fig. 1). The bedrock that underlies the diamond-bearing alluvium comprises Palaeozoic orogenic complexes of the Lachlan Fold Belt (e.g. Collins and Vernon, 1992), and the Mesozoic orogenic New England Fold Belt, east of the Lachlan (e.g. Roberts and Engel, 1987). The Lachlan Fold Belt is a north–south trending 2,000 km long, 700 km wide complex of accreted terranes, extending from New South Wales through Tasmania. The New England Fold Belt is interpreted as representing terranes that docked in two stages in the late Carboniferous to early Permian and in the late Permian to middle Triassic, and contains exposures of ultramafic rocks, eclogites and blueschists (e.g. Allan and Leitch, 1990).

The Wellington alluvial diamonds occur in the Macquarie River drainage system within the early to mid-Palaeozoic Lachlan Fold Belt, and are reworked from deep leads. Heavy minerals associated with the diamonds at Wellington include abundant topaz, corundum (small sapphires and rubies) and gold.

Methods

The physical characteristics of more than 500 alluvial diamonds from Wellington, NSW, were studied by a number of methods that include surface studies, internal structures using cathodoluminescence and birefringence, N impurity characteristics from infrared (IR) microscope measurements of cut and polished plates, *in situ* electron microprobe analysis of mineral inclusions, and C isotope analysis of diamond pieces.

One hundred and fifteen diamonds were cut by laser and polished to expose inclusions and produce plates using the laboratory facilities at Argyle Diamonds, Perth. Polishing of laser-cut plates was also carried out at the Yakutian Science Institute, Yakutsk, Siberia, and Protea Diamonds, Sydney. The (110) orientation was preferred in the polishing of centrally sectioned diamond plates except in the case of diamond that contained inclusions, where the surface nearest to the inclusion was polished. In the course of the study we found that the orientation of the plate was not critical in deciphering the growth morphology of the diamond by birefringence and cathodoluminescence.

Morphological features of diamonds were studied with a binocular microscope (Nikon SMZ-2T) and Scanning Electron Microscope (SEM) Jeol JSM-840 using an accelerating voltage of 6.0 kV and working distance of 15 mm. Surface structures are described using the terminology of Orlov (1977), Robinson (1980) and Robinson *et al.* (1989) where possible.

Cathodoluminescence characteristics of 80 diamond plates and polished faces were studied using Cambridge Instruments Cold Cathode Luminescence (CITL CCL 8200 Mk3) microscopes, and a Nuclide Luminoscope cathodoluminescence attachment for the optical microscope. Accelerating voltages of 12–15 kV and an electron beam current of ~0.5 mA were used.

Nitrogen contents and aggregation states were calculated by the methods outlined in Mendelssohn and Milledge (1995) using spectra measured with a Bruker IR microscope attached to an IFS45 optical bench operated with an aspect computer, and Digilab FTS-60A with a UMA-300A microscope attachment. Spectra were recorded in the mid-IR range (4000–650 cm^{-1}) from 84 scans (Bruker) and 64 scans (Digilab), at a resolution of 8 cm^{-1} with a beam aperture of ~90 μm. A liquid nitrogen attachment was used to cool the detectors. Spectra were analysed using Bruker OPUS IR-W (version 2.2).

Electron microprobe analyses of mineral inclusions were carried out using a Cameca SX50. The accelerating voltage was 15 kV for silicate, and 20 kV for sulfide minerals. The sample current was 20 nA and beam width ~3 μm. The standards were a mixture of natural and synthetic minerals and the Pouchou and Pichoir (1984) method was used for matrix corrections.

Carbon isotope analyses were determined at the Centre for Isotope Studies, CSIRO, North Ryde. Fragments of diamond weighing ~1 mg were

placed into a previously cleaned 6 mm quartz glass tube (10 cm long) together with 10–20 mg of conditioned CuO agent. Tubes were evacuated, sealed and reacted in a furnace at 1000°C for 5 h. The CO_2 produced by oxidation of the diamond was separated cryogenically from other gases and collected in a gas sample tube for mass spectrometric analysis on a Finnigan 252 mass spectrometer using dual inlet mode. An internal anthracite standard ($\delta^{13}C = -23.1$ PDB) was run with each batch and international graphite standard NBS21 ($\delta^{13}C = -28.1$ PDB) was analysed at regular intervals. Reproducibility is typically $\pm 0.1‰$.

Morphological features of diamonds from Wellington, NSW

The Wellington diamonds from NSW can be divided into two discrete groups on the basis of morphology, here termed Group A and B. Distinctions in suites of mineral inclusions, C isotopes and growth structures were recognized between the two groups following this initial separation. Group A diamonds are typical of those from Airly Mountain (Fig. 1) and Group B diamonds are similar to diamonds dominating the population at the Copeton and Bingara localities (Fig. 1). In this study, Group A predominates over Group B at the ratio of 4:1. However a higher proportion of the Group B diamonds have been recorded at Wellington (Joris, 1983). Groups A and B diamonds are distinguishable by shape, etch structures and deformation characteristics (Table 1). Morphological features common to the two groups are outlined below: (1) the sizes range between 0.1 and 1.2 carats; with a mean of 0.17 carats; (2) the colours are pale yellow, yellow, brown and white in decreasing order of abundance; (3) most stones (~85%) show heavy resorption with no preservation of

TABLE 1. Summary of morphological, mineral inclusion, growth, N content, N aggregation state and C isotope characteristics of the Group A and Group B diamonds from Wellington NSW

Characteristics	Group A	Group B
Size, form, colour	~0.17 carats; tetrahexahedral and dodecahedral; 35% twinned Straw to pale yellow, white and brown	~0.17 carats; Flattened, elongate or regular dodecahedra; Brown white (Group B1), straw, pale yellow (Group B2),
Surface characteristics	85% Class 1 resorption, 1–55% preservation 15% Class 4 to 2, 85 to 62.5% preservation Low relief surfaces Elongate drop hillocks Widely spaced shield shaped laminae Corrosion sculpture with micro hexagonal pits Fan-like striations with wedge-shaped micro pits Microdisk sculpture and polished	All Class 1 resorption, ~1–55% preservation Low relief polished surfaces Pitted hemispherical cavities Abundant deformation seams Ring pits Group B1 strain hillocks
Deformation	40% Glide planes shagreen	95% Deformation lamellae
Abrasion	Percussion scars and fine frosting	Fine frosting and fractured points and faces Low-N stones, strain elongate hillocks
Radiation damage	Abundant green and brown spots (30%)	Rare green and brown spots
Internal growth structure	75% octahedral: (includes 25% multiple octahedral and 5% cubo-octahedral centres); 20% homogeneous; <5% sector	50% non-planar with strain: Group B1 50% homogeneous; Group B2
Nitrogen characteristics	Group A1: 90%; 250–2500 ppm N; 6–42% IaB Group A2: 10%;140–900 ppm N; 44–95% IaB N rich centres, N poor rims (33% Type II rims)	Group B1: <400 ppm N; <12% IaB Group B2: 900–2800 ppm N; 33–65% IaB
Paragenesis	Peridotitic (P) with minor eclogitic (E) P = Olivine, pentlandite, wüstite E = omphacite, garnet	Eclogitic Omphacite, diopside, coesite, garnet, sulfide
Carbon isotopes ($\delta^{13}C$)	−9.8 to −3.1‰ (34), −23‰ (1)	−0.9 to +2.9‰ (8), −5‰ (1)

primary octahedral or cube growth forms, and with half or less than half of their original volume preserved (Class 1 resorption of Robinson *et al.*, 1989); (4) the surfaces have low relief etch structures and were chemically polished at a late stage in their resorption histories; (5) most diamonds show evidence of abrasion from transportation subsequent to resorption and original emplacement, with finely abraded or broken edges and points, and percussion scars. Abrasion is more pronounced for Group B stones; (6) radiation damage was observed on ~30% of all Wellington diamonds with Group A diamonds showing greater damage.

Morphology of Group A diamonds

Group A diamonds preserve resorbed tetrahexahedroid and dodecahedral forms with greater surface relief than those of Group B. One third of the stones show twinning with flattened forms and <10% of diamonds are aggregate forms. Secondary resorption surface structures of most Group A diamonds include large transverse drop-shaped hillocks and shield-shaped laminae with one dominant, widely spaced lamina around each six-fold axis (Fig. 2*a*). There is some correlation between colour and morphological characteristics. The majority of the population of straw to pale yellow or white colour, preserve glossy surfaces with low relief structures. Some stones have concave points with tetragonal pits, suggesting a cubic growth influence or preferential etching in the cubic (100) orientation. About one third of the population, consisting of pale brown, white and pale yellow stones, has corroded faces with uniformly sculpted micro-etch hexagons that have been rounded by later resorption events. A small group of white stones has retained central octahedral faces (Class 2 to 4 resorption category; Robinson *et al.*, 1989), with negative trigonal pits.

The surfaces of most Group A stones show evidence of two etch episodes overprinting earlier

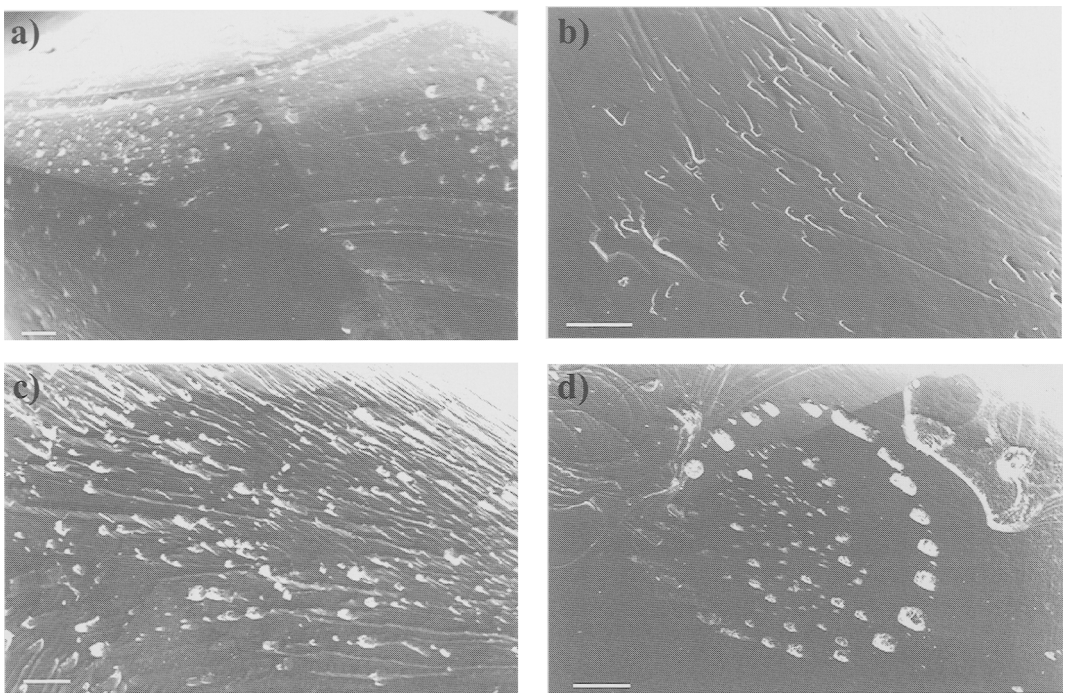

FIG. 2. Scanning microprobe images of diamond surfaces: scale bars are 100 μm. (*a*) Wellington Group A diamond with widely spaced dissolution laminae. (*b, c*) Group A diamonds with fan-like striations attached to micro-pits on tetrahexahedroid faces. Striations fan from the four-fold axes and terminate at the median line of the dodecahedral face. (*d*) Resorbed low relief dodecahedral faces of a Group A diamond with a circular array of micro-pits adjacent to microdisk structure.

etch structures on secondary dodecahedral faces: (1) fan-like striations attached to micro-pits; and (2) microdisk sculpture. Fan-like striations attached to micro-pits (Figs 2*b,c*), a feature not previously described for any diamond, are observed on the surfaces of 25% of Group A diamonds. Striations fan from the four-fold axes of the tetrahexahedroid and terminate at or before reaching the median line of the tetrahexahedroid face, cutting across growth layers. Where they terminate, the striations develop into wedge-shaped micro-pits. Micropits that intersect the octahedral (111) and cube (100) surfaces have trigonal, hexagonal or tetragonal form respectively, indicating a crystallographic influence on the shape of the etch pits.

Microdisk sculpture is also common to the surfaces of the majority of Group A diamonds and postdates the development of fan-striations attached to micro-pits. This structure shows an array of superimposed disks. The disks decrease in size with increasing topography and may have formed because attached bubbles protected small surface areas on the stones during resorption (Robinson, 1980). One diamond shows a spiral outline of micro-pits adjacent to microdisk structures (Fig. 2*d*). A possible inference is that the two etch structures are related (Robinson, 1980). Similar structures have been recorded on diamonds in placer deposits (e.g. Phuket, Thailand; Sunagawa *et al.*, 1983) and diamonds *in situ* in kimberlites (e.g. Premier Mine, South Africa; Mendelssohn *et al.*, 1983).

Group A diamonds with very low surface relief show microdisk sculpture grading to ring-pits with less relief. This suggests that ring-pits are the low relief or more resorbed equivalent of microdisk sculpture. Microdisk sculpture and ring-pits are also a common characteristic of the Group B diamond surfaces.

One third of Group A diamonds show evidence of deformation, and about half of the deformed diamonds are brown. The brown colour may be due to precipitation of graphite along slip-plane dislocations (Robinson *et al.*, 1989). Deformation indicators include lamination lines, that cross-cut the stones in more than one cleavage direction, and micro-hillocks formed by the intersection of lamination lines with a second set of lamination lines (shagreen texture; Robinson, 1980). The deformation textures in these diamonds are similar to plastic deformation described for kimberlitic and related diamonds worldwide (e.g. Harris, 1992).

Morphology of Group B diamonds

Group B diamonds are characterized by flattened or elongate irregular dodecahedral forms. Twinned and aggregate forms are rare. Diamonds have glossy surfaces and are strongly rounded by resorption (in some cases secondary dodecahedral faces are not discernible). Group B diamonds can be divided into two approximately equal groups based primarily on colour: white and pale brown stones (Group B1) and straw to pale yellow stones (Group B2). Differences between the two groups include resorption features, internal growth structures, N concentrations and evidence of deformation (see section below on internal growth structures).

All Group B diamonds are characterized by three distinct surface features: (1) low relief, chemically polished faces with mico-ring pits; (2) abundant, partially developed deformation laminae; and (3) pitted hemispherical cavities (Robinson, 1980). Low relief polished faces host micro ring-pits of varying size (4–72 μm; Fig. 3*a,b*). Superposition of ring pits of varying sizes on the polished diamond surfaces, similar to microdisk sculpture, suggests the influence of fluid or gas bubbles as noted above. Ring pits on low relief polished surfaces have also been observed on some of the Group A diamonds, although these diamonds generally preserve more surface relief in the form of micro-disk sculpture. In rare cases the Group B diamonds preserve microdisk sculpture.

Group B diamonds show strong deformation laminae oriented in multiple cleavage directions that may be only partially developed through the stone. Under cathodoluminescence these lamellae appear to be confined to inner regions typified by deformed textures. Group B1 preserve positive herringbone-like structures along deformation lineations, revealing less resorbed primary growth layers along displaced surfaces (Figs 3*c,d*). These diamonds also host clusters of small hillocks that are confined to surface areas correlating with the internal regions with greatest strain (Fig. 3*c*). A similar observation was made by Orlov (1977). Group B2 diamonds have less surface relief, rarely show evidence of herringbone structure and preserve mostly linear features (Fig. 3*e*).

Pitted hemispherical cavities (between one and twenty cavities per stone) are large isolated depressions with frosted bases (Fig. 3*e*). In the Group B1 stones pits are less abundant, deeper and preserve more crystallographic form with hexagonal, cubo-octahedral and tetragonal depressions.

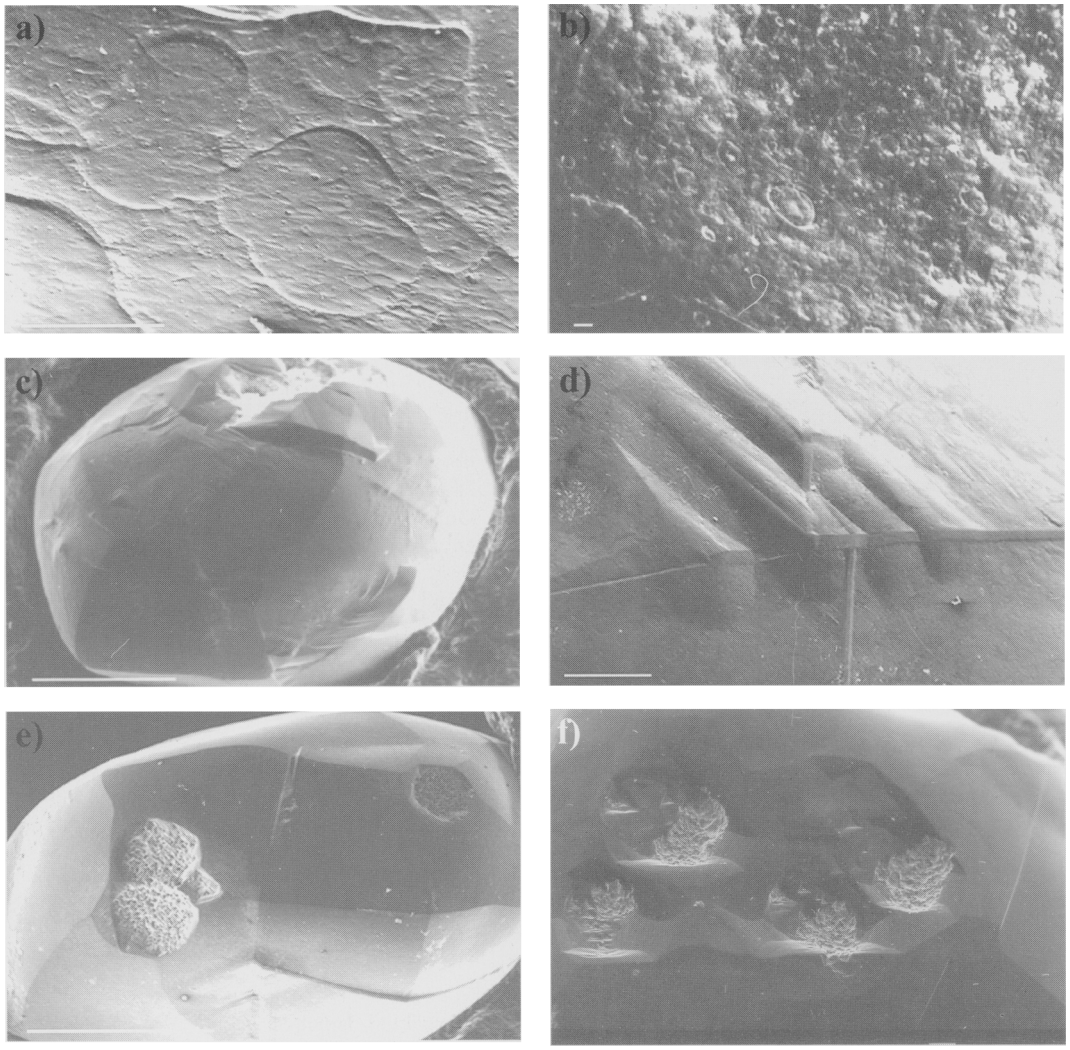

FIG. 3. Scanning microprobe images of diamond surfaces: scale bars are 100 μm except for 3*b* (10 μm), 3*c* and 3*e* (1 cm). (*a,b*) Wellington Group B diamonds with low relief polished surfaces and micro ring pits. *a* shows ring-pits overprinting microdisk structures. (*c,d*) A Group B1 diamond showing partially developed deformation seams oriented in several cleavage directions with herringbone structures. Micro-hillocks occur in zones of most strain. (*e*) A Group B2 diamond with pitted hemispherical cavities and deformation lamellae with linear structures oriented in two cleavage directions. (*f*) Pitted hemispherical cavities formed by the corrosion of former etch trigons on inverted octahedral (111) surfaces adjacent to an isolated deformation seam (running north–south).

The Group B2 diamonds show less surface relief than the Group B1 diamonds and preserve shallow rounded pits. The Group B1 stones show evidence of greater internal strain and inhomogeneity: they have deeper etch pits, preserve herringbone displacement structures along deformation laminae and contain strain hillocks.

Significance and interpretation of main morphological features

Microdisk sculpture

Both Group A and Group B diamonds show microdisk sculpture that developed late in their resorption histories and both groups share characteristic polished surfaces due to resorption.

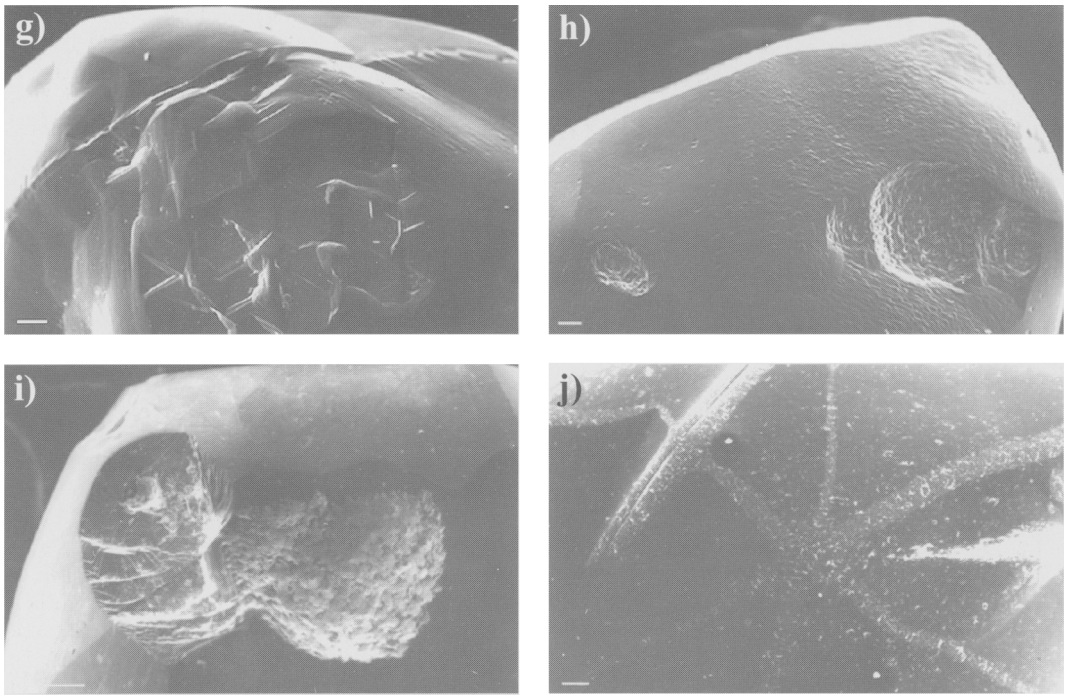

FIG. 3 (*cont.*) (*g*) A Group B diamond with hexagonal etch pits on an octahedral (111) surface that have avoided being corroded as they have been in Fig. 3*f*. (*h*) A large cavity with a corroded surface preserved on an inverted and less resorbed face of a Group B diamond. Non-inverted faces are polished and have experienced more resorption. (*i*) Evidence of two stages of development of adjacent pitted hemispherical cavities formed from mineral inclusion pits. The left cavity is a newly formed inclusion pit postdating the diamond's resorption history. The right cavity with a frosted base is similar in size and form to the left cavity suggesting that it is also an inclusion pit that formed during processes of late stage resorption. (*j*) A Group B diamond with fine abrasion features showing network cracks that are most strongly developed on protruding surfaces such as crystal edges and deformation laminae (top left).

We conclude that microdisk sculpture records part of the process producing the 'chemical polish' that gives both diamond groups their glossy surfaces. The chemical polish observed on these diamonds is similar to that seen on diamonds from the Ellendale lamproites (Hall and Smith, 1985). A similar lustrous polish on diamond surfaces can be created in Na_2CO_3 at $\sim$800°C (Mahlzahn, 1997), suggesting that the more alkaline composition of lamproites may be the reason for such polishing in lamproitic *vs* kimberlitic magmas.

Plastic deformation

Deformation features in diamond are typically characterized by parallel laminae cutting growth surfaces, mostly visible on resorbed surfaces (Harris, 1992). Deformation characteristics in the Group B diamonds are unique in that deformation lamellae occur as a few isolated and commonly partially developed linear features which occur along multiple cleavage orientations, creating irregular forms. The characteristic toughness of these diamonds (Joris, 1983) is attributed to deformation laminae.

Pitted hemispherical cavities

The pitted hemispherical cavities formed late in the diamonds' resorption history. They are inferred to have formed in three different ways: (*a*) by corrosion of former etch pits, e.g. trigons etc. (Fig. 3*f,g*); (*b*) as a corrosion structure preserved on inverted faces and pits of a crystal with more protruding surfaces subsequently polished in the later stages of resorption (Fig. 3*h*); and (*c*) by corrosion of pits formerly occupied by mineral inclusions (Fig. 3*i*). The

corrosion feature developed on the newly exposed inclusion pit during a late stage of resorption, differentially attacking the lesser resorbed faces. Pitted cavities probably developed at the same time as the late stage chemical polish. However, the inverted, less resorbed surfaces where the pits formed, etched differently either because they were protected or because the etch substrate affected less resorbed or weaker surfaces differently. Three different mechanisms are discussed below.

(*a*) We interpret pitted hemispherical cavities to be crystallographically controlled etch pits that are surface expressions of large dislocations (Lang, 1964, Sunagawa *et al.*, 1984). The SEM images show that the bases of the pits are uniformly etched with micro-trigons, hexagons and tetragons, while the corroded pits are central to larger etch structures such as trigonal or hexagonal pits. The pitted cavities also occur in the centres of large pre-existing etch structures that are also crystallographically controlled by dislocations. The common occurrence of pitted hemispherical cavities adjacent to or superimposed on the abundant deformation lineations in the Group B diamonds suggests that both growth and strain dislocations are sites of preferred etching (Fig. 3*e*–*g*).

(*b*) Some Group B diamonds show not only isolated pitted hemispherical cavities etched with micro-pits, but also depressed crystal faces which exist because of the irregular primary crystal forms. This suggests that corrosive etching was not only localized to areas of isolated crystal defects, but affected whole diamond surfaces prior to chemical polishing. Inverted faces and etch pits hosting pitted cavities were not affected by the later polishing event. The pits and negative faces may have escaped polishing in the final stages of resorption because the surface was protected. Alternatively the protected and less resorbed faces (e.g. remnant cube (100) and octahedral (111) surfaces) etched differently during the final polishing event and were corroded whilst resorbed dodecahedral faces were polished (Fig. 3*h*).

(*c*) It is possible that some of the pitted hemispherical cavities represent former inclusion pits (Fig. 3*i*), as proposed by Meyer *et al.* (1995) based on the occurrence of a coesite grain in a pitted hemispherical cavity. We found it difficult to polish these diamonds to expose large inclusions because the inclusions often burst from the diamond or the stone fractured just before they were exposed. Presumably a similar escape of the inclusion may have happened during resorption. Further resorption may have frosted the inclusion pits. Barron *et al.* (1994, 1996) suggested that the pits are negative imprints of garnet and other mineral grains that grew with the diamonds in a solid state. However, this is unlikely as the shapes of the pits do not reflect the shapes of the mineral inclusions preserved in these stones and the observed features favour a resorption origin.

Etch structures

Textural relationships between surface etch structures in the Group B diamonds indicate at least three episodes of resorption: (1) resorption of irregular, deformed octahedra and cubo-octahedra forms resulting in flattened dodecahedral forms with the development of large trigonal, tetragonal or hexagonal etch pits at the intersection of dislocations with planar growth surfaces; (2) corrosive resorption that either attacked local areas of crystal defect or weakness (overprinting etch trigons, hexagons and tetragons with the development of pitted cavities) or affected the whole surface (resulting in an overall pattern of micro-trigons and hexagons on all crystal faces, including former etch pits and inverted faces that are corroded out to form pitted hemispherical cavities); and (3) late-stage chemical polishing to glossy surfaces and rounded forms, and the preservation of pitted hemispherical cavities on inverted etch pits and unpolished faces, possibly preserved because of protection by a graphite coat, or differential resorption on less resorbed primary growth surfaces.

Radiation and mechanical damage

Radiation damage is observed as green and brown spots (in approximately equal proportions) in ~40% of the Group A diamonds and is evident under cathodoluminescence as black spots with yellow radiation haloes in the majority of Group A and extremely rarely in the Group B stones. Radiation damage indicates contact with U and Th-bearing minerals. Alpha-particle damage to diamond is calculated to take ~10 Ma to form in an alluvial environment (Vance and Milledge, 1972). The change from green spots to brown has been shown experimentally to be a function of temperature (>600°C) and hence a significant time is required for this colour change at the earth's surface (Vance *et al.*, 1973). Some of the

Wellington diamonds have both green and brown spots on a single stone. This suggests that the stone was exposed to U, Th radiation at different times.

Two types of mechanical abrasion are observed on surfaces of the Group A and Group B diamonds: (1) heavy abrasion with percussion scars, fractured points, edges and faces, or fracturing along planes of weakness such as deformation seams; and (2) fine abrasion with rounding of edges and protruding features creating a finely frosted network texture (Fig. 3*j*). The Group A diamonds show mostly fine abrasion structures and the Group B stones show both heavy and fine structures. We can thus infer that Group B diamonds at Wellington travelled over longer distances, or in a higher energy environment, than Group A stones.

Mineral inclusions

Background

Diamonds worldwide can be divided into two main groups based on mineral inclusions: peridotitic and eclogitic (e.g. Meyer, 1987). The peridotitic paragenesis includes minerals of ultramafic association, with Ni-rich sulfides (NiO > 8%), forsteritic olivine, chrome-pyrope garnet, chrome spinel, orthopyroxene and chrome-diopside. Minerals of the eclogitic paragenesis include pyrope-almandine garnet, omphacite, coesite, rutile and Ni-poor sulfides (Meyer, 1987; Bulanova *et al.*, 1996).

Previous studies of the mineral inclusions in eastern Australian diamonds have focused on stones from the Copeton field and indicated they belonged to the eclogitic/calc-silicate paragenesis. Rare olivine inclusions of the peridotitic paragenesis were also described (Sobolev *et al.*, 1984). Earlier studies of eastern Australian diamond inclusions have noted the lack of sulfide, spinel, ultramafic and eclogitic garnet inclusions (Meyer *et al.*, 1995). In the Wellington diamonds, the eclogitic inclusions have a broad compositional range including a suite characterized as a "calc-silicate paragenesis" (Sobolev *et al.*, 1984) comprising diopside coexisting with grossular-almandine garnet with a high Ti and Na content, and coesite.

Inclusions of the calc-silicate paragenesis are mostly restricted to diamonds from the Copeton locality (Sobolev *et al.*, 1984; Meyer *et al.*, 1997). Griffin *et al.* (1998) showed that this paragenesis is just an end-member of a compositional spectrum of eclogitic mineral compositions. Trace element data for these calc-silicate inclusions from the Copeton diamonds show that compared to other mantle-derived garnet and clinopyroxene (O'Reilly and Griffin, 1995), the 'calc-silicate' garnets are rich in Zr and Ti, and are very low in Y while the clinopyroxenes are high in Ni and low in Sr (Griffin *et al.*, 1998).

Inclusions in the Wellington diamonds

Forty-eight syngenetic mineral inclusions with compositions of the peridotitic or eclogitic/calc-silicate paragenesis, were analysed *in situ* from 39 polished Wellington diamonds. A good correlation was found between mineral inclusion paragenesis and the two diamond groups. The 33 inclusions in Group A diamonds are mostly of the peridotitic paragenesis (Table 2) with the exception of three that are eclogitic. All Group B diamond inclusions are of the eclogitic/calc-silicate paragenesis (Table 3).

Peridotitic paragenesis

The Group A diamonds contain inclusions of olivine, pentlandite, wüstite and chromite. Eighteen forsterite inclusions were exposed from seventeen Group A diamonds and have compositions between $Fo_{91.8}$ and $Fo_{95.3}$ with a mean of $Fo_{93.0}$. The range in values suggests that the inclusions are both from the lherzolitic and harzburgitic fields, with the mean value in the harzburgite field. The major element compositions of these inclusions are similar to olivine inclusion compositions from worldwide occurrences (Table 2; Meyer, 1987).

Two pentlandite inclusions with >16 wt.% NiO also belong to the peridotitic paragenesis (Bulanova *et al.*, 1996). Wüstite and Ni-Fe-Cr alloy inclusions occur as small central inclusions in several diamonds, and are analogous to central seed structures observed in peridotitic-suite diamonds from Siberia (Bulanova *et al.*, 1998).

Eclogitic/calc-silicate paragenesis

The Group B diamonds contain inclusions of omphacite, diopside, coesite, garnet and sulfide. Three Group A inclusions are also eclogitic: two garnet and one omphacite. Nine eclogitic clinopyroxene inclusions recovered from six diamonds have jadeite compositions with a discontinuous range between 8 and 40 mol.% Jd (Table 3; Fig. 4). The compositions bridge the diopside–omphacite solid solution. The range is greater than previously recorded for eclogitic clinopyr-

TABLE 2. Electron probe data for syngenetic peridotitic mineral inclusion compositions in diamonds from Wellington

Population	C-B	C-B	A	A	A	A	A	A	A	A	A	A	A	A	A	A	A	A	A	A	A
No. Anal.	1	1	2	1	1	1	1	1	1	1	1	1	2	1	2	2	3	1	3	2	1
Sample	AS-11	AR-17	W1	W44	W7	W84	W86 (1)	W86 (2)	W94	W144	W190	W204	W209	W223	W224	W226	W228	W231	W233	W248	W238
	Olivine	Olivine	Olivine	Olivine	Olivine	Olivine	Olivine	Olivine	Olivine	Olivine	Olivine	Olivine	Olivine	Olivine	Olivine	Olivine	Olivine	Olivine	Olivine	Olivine	Chromite
SiO_2	41.00	41.50	41.92	40.30	43.30	41.57	40.61	40.30	40.00	41.06	40.95	41.98	40.13	40.24	40.54	41.07	40.93	41.20	41.46	41.11	0.13
TiO_2	0.01	0.00	0.01	0.00	0.02	0.03	0.00	0.02	0.02	0.01	0.02	0.00	0.00	0.00	0.01	0.02	0.01	0.03	0.02	0.00	0.19
Al_2O_3	0.01	0.00	0.01	0.02	0.01	0.01	0.00	0.04	0.00	0.00	0.00	0.06	0.01	0.01	0.02	0.01	0.02	0.00	0.01	0.02	6.44
Cr_2O_3	0.05	0.06	0.03	0.11	0.05	0.04	0.09	0.07	0.03	0.10	0.06	0.06	0.11	0.12	0.10	0.08	0.08	0.00	0.09	0.07	63.38
FeO	7.41	6.57	6.65	7.25	4.82	7.95	5.81	5.99	7.34	7.51	7.08	6.41	7.79	7.98	6.65	7.50	6.59	5.50	7.88	5.84	14.65
MnO	0.10	0.00	0.09	0.11	0.03	0.15	0.00	0.05	0.08	0.06	0.08	0.01	0.05	0.06	0.07	0.11	0.08	0.07	0.11	0.09	0.00
MgO	49.90	50.60	52.26	52.37	54.85	49.05	50.46	50.23	50.39	50.76	51.32	51.30	49.96	49.79	50.85	51.38	51.01	52.77	51.18	52.30	13.56
CaO	0.01	0.00	0.06	0.02	0.03	0.09	0.01	0.00	0.03	0.07	0.04	0.04	0.04	0.04	0.03	0.01	0.01	0.05	0.02	0.00	0.00
Na_2O	0.00	0.00	0.00	0.00	0.02	0.02	0.04	0.01	0.01	0.03	0.01	0.02	0.01	0.00	0.02	0.00	0.01	0.00	0.01	0.00	0.02
K_2O	0.00	0.00	0.00	0.00	0.01	0.01	0.01	0.00	0.00	0.00	0.00	0.04	0.02	0.03	0.01	0.02	0.01	0.00	0.00	0.02	0.01
NiO	0.31	0.34	0.42	0.49	0.28	0.33	0.37	0.29	0.42	0.55	0.34	0.41	0.33	0.38	0.37	0.35	0.29	0.32	0.38	0.35	0.09
Total	98.80	99.07	101.44	100.68	103.42	99.22	97.40	97.00	98.32	100.16	99.88	100.33	98.46	98.65	98.66	100.53	99.04	99.95	101.17	99.80	98.47
Mg No.	0.92	0.93	0.93	0.93	0.95	0.92	0.94	0.94	0.92	0.92	0.93	0.93	0.92	0.92	0.93	0.92	0.93	0.94	0.92	0.94	0.62

Population	A	A		A	A
No. Anal.	5	3		1	2
Sample	W92	W119		W18	W6
Si	0.05	0.05	Si	2.32	0.50
Al	0.01	0.01	Ti	0.00	0.01
Cr	0.39	0.36	Al	0.03	0.10
Fe	42.59	34.98	Cr	0.36	0.57
Mn	0.038	0.01	Fe	98.77	97.61
Cu	0.53	0.88	Mn	0.30	0.33
Zn	0.03	0.02	Mg	0.00	0.00
Ni	16.96	22.17	Ca	0.01	0.02
S	35.19	36.16	Na	0.01	0.06
O	4.62	2.02	K	0.02	0.02
			Ni	0.19	0.13
Total	100.41	96.67	Total	102.01	99.34

TABLE 3. Electron probe data for syngenetic eclogitic mineral inclusion compositions in diamonds from Wellington, including garnet analyses from the Copeton field (C–B; after Sobolev *et al.*, 1984).

Population	A	A	B	C-B	C-B	A	B	B	B	B	B	B	B	B
No. Anal.	1	1	2			1	1	3	3	1	2	5	3	1
Sample	W22	W193	W171	AR-21	AR-36	W11	W10	W43	W80	W83 (1)	W83 (2)	W79 (1)	W79 (2)	W79 (3)
Mineral	Garnet	Garnet	Garnet	Garnet	Garnet	Omph.	Omph.	Omph.	Omph.	Omph.	Omph.	Diop.	Diop.	Diop.
SiO_2	40.68	38.19	40.59	39.00	39.30	54.87	55.86	54.26	55.53	55.51	55.59	54.48	54.61	55.10
TiO_2	0.06	0.34	1.47	1.79	1.44	0.24	0.43	0.70	0.60	0.56	0.57	0.13	0.15	0.14
Al_2O_3	23.19	22.44	20.99	20.00	21.00	10.49	5.59	9.10	8.71	8.98	9.06	2.88	2.71	2.83
Cr_2O_3	0.00	0.08	0.07	0.09	0.19	0.02	0.00	0.05	0.03	0.08	0.08	0.43	0.42	0.39
FeO	10.47	13.83	3.30	6.22	2.92	3.68	6.14	6.83	5.92	6.15	6.04	2.13	2.33	2.22
MnO	0.00	0.15	0.08	0.15	0.00	0.06	0.00	0.08	0.03	0.05	0.08	0.03	0.05	0.02
MgO	11.25	6.81	2.63	2.83	1.91	9.14	15.46	8.43	9.42	8.64	8.57	15.32	15.29	15.59
CaO	15.72	17.17	30.67	28.70	32.40	14.33	12.82	15.88	16.74	15.18	15.32	23.24	23.00	22.58
Na_2O	0.00	0.15	0.20	0.30	0.22	5.70	3.51	3.91	3.07	4.86	4.95	1.19	1.14	1.06
K_2O	0.00	0.04	0.00	0.00	0.00	0.36	0.16	0.32	0.55	0.33	0.36	0.12	0.09	0.20
NiO	0.00	0.02	0.01	0	0	0.00	0.00	0.04	0.00	0.01	0.05	0.04	0.03	0.07
Total	101.37	99.22	99.98	99.08	99.38	98.89	99.97	99.60	100.60	100.35	100.67	99.99	99.82	100.20
Mg#	0.66	0.47	0.59	0.45	0.54	0.82	0.82	0.69	0.74	0.71	0.72	0.93	0.92	0.93
Gr	0.40	0.46	0.83	0.77	0.87									
Pyr	0.40	0.25	0.10	0.11	0.07									
Alm	0.21	0.29	0.07	0.13	0.06									
Jd						0.423	0.330	0.316	0.255	0.375	0.377	0.086	0.084	0.080
Di+Hd						0.552	0.670	0.675	0.770	0.631	0.623	0.899	0.901	0.914
CaTs						0.025	0.000	0.009	0.000	0.000	0.000	0.015	0.015	0.006

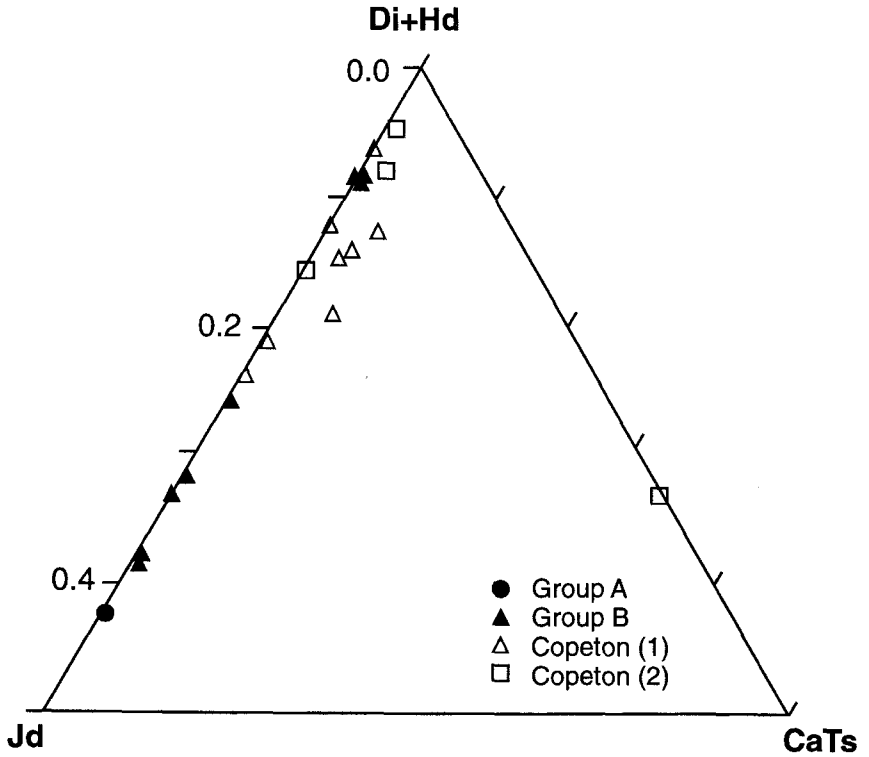

FIG. 4. Composition of clinopyroxene inclusions in NSW diamonds, shown in proportions of diopside+hedenbergite, jadeite and Ca-Tschermak's molecule. Clinopyroxene inclusions in diamonds from the Copeton field are similar to Group B from Wellington. Copeton (1) and (2) correspond to the data of Sobolev *et al.* (1984) and Meyer *et al.* (1997) respectively.

oxenes from the Copeton diamonds (4–24 mol.% Jd; Sobolev *et al.*, 1984; Meyer *et al.*, 1997). The combined data show a continuous range of jadeite contents from diopside to omphacite which illustrate that the 'calc-silicate' inclusion suite is simply an end-member component of a broader range of compositions. The single omphacite found in a Group A diamond has the highest jadeite content (40 mol.%). The highest jadeite content for the Group B diamonds is 39 mol.%.

Omphacite inclusions in the Wellington diamonds overlap representative analyses of omphacite from worldwide data (Meyer, 1987). However they tend to be more diopsidic and similar in composition to those reported from Copeton. Five coesite inclusions were found in three diamonds. Garnet occurs as inclusions in three diamonds: one garnet inclusion from a Group B diamond is grossular-rich (77%) with high Ti and Na, and low Fe contents and a composition similar to garnet previously reported from the Copeton field (Table 3; Sobolev *et al.*, 1984). This garnet contains an inclusion of a low-Ni sulfide. The two eclogitic garnets found in Group A diamonds plot within the range of eclogitic garnets from worldwide data with moderate mixes of grossular, almandine and pyrope molecules.

Carbon isotopes

Carbon isotope ratios for diamonds worldwide in general show a correlation with their paragenesis. Peridotitic diamonds have a relatively narrow $\delta^{13}C$ range (−10‰ to 0‰) with an average of ~ −6‰ (e.g. Kirkley *et al.*, 1991). The eclogitic range is more dispersed ($\delta^{13}C$ −34 to +3‰) with an average of ~-5‰ (e.g. Kirkley *et al.*, 1991).

Thirty-four Group A diamonds overlap the main distribution of peridotitic and eclogitic diamonds from world wide occurrences, with the $\delta^{13}C$ ranging from −9.8 to −3.1‰. One stone has a $\delta^{13}C$ of −23.2‰. Group A diamonds with peridotitic inclusions show a $\delta^{13}C$ range of −6.7 to −3.1‰ (Fig. 5).

$d^{13}C$ values for Wellington Group A diamonds are similar to values known for morphologically similar diamonds from Airly Mountain, NSW. These values are $\delta^{13}C = -9$ and −3‰ ($n = 5$; Sutherland *et al.*, 1994); and $\delta^{13}C = -10$ to −4‰ for an unknown number of stones (Meyer *et al.*, 1997).

Sobolev (1985) reported 44 C isotope analyses of diamonds from the Copeton localities showing a range between $\delta^{13}C$ −3.3‰ to +2.4‰. The lightest recorded value of these stones was olivine-bearing and thus peridotitic. Nine Group B diamonds have $\delta^{13}C$ values between −0.9 and +2.9‰ except for one Group B diamond containing an omphacite inclusion which has a $\delta^{13}C$ of −5.4. Other Group B diamonds with eclogitic inclusions have a $\delta^{13}C$ range between +0.1 and +2.1 ‰ (Fig. 5).

Nitrogen contents and growth patterns

The internal structures of diamond record evidence of the history of growth, dissolution and deformation during mantle residence. Molecular impurities incorporated in diamond (mainly N) exhibit variation between growth layers and these may be revealed across different zones by cathodoluminescence and birefringence microscopy of polished central plates. In this study, images of internal structures have also been used to provide a spatial context for the interpretation of N content and aggregation states measured by IR spectroscopy.

The Wellington diamonds are characterized by blue cathodoluminescence, indicative of abundant N. Zones of dark or no cathodoluminescence indicate trace amounts or an absence of N. Yellow cathodoluminescence colours are less common, and do not appear to indicate incorporated impurities. Rather, they occur in zones with low N contents, such as amorphous seeds (commonly H-bearing), around mineral inclusions and radiation spots, and along deformation laminae.

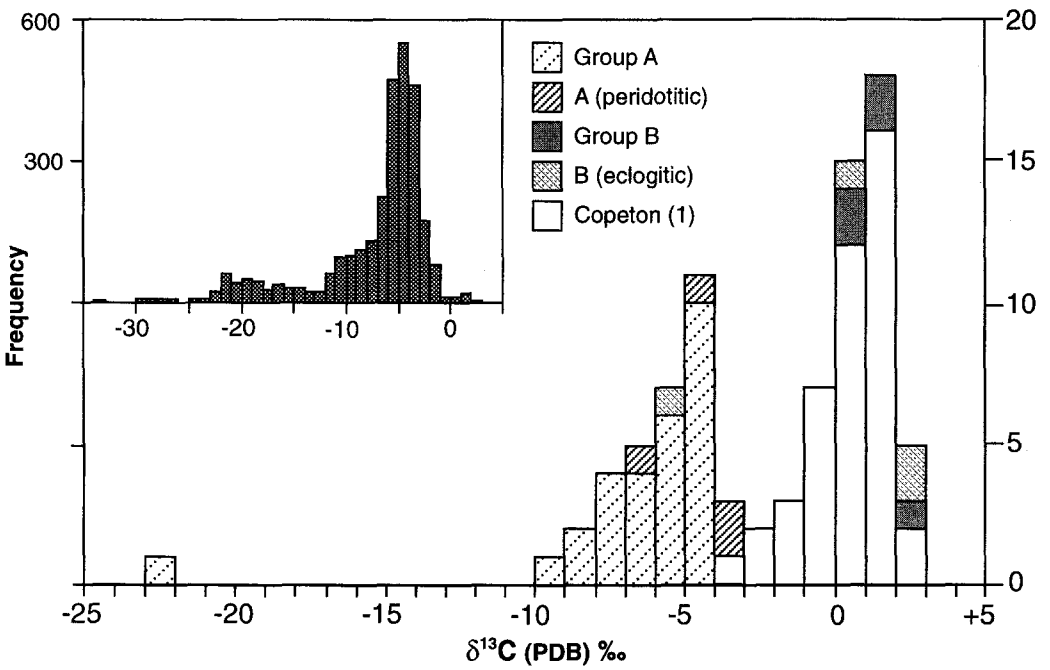

FIG. 5. Carbon isotope ratios and distribution for diamonds from New South Wales, compared with the world-wide distribution (inset; after van Heerden *et al.*, 1995). The data for Copeton (1) are analyses from Sobolev (1985). The Wellington data are grouped by paragenesis and morphological groups (A and B), discussed in text.

Growth characteristics of Group A diamonds

Concentric octahedral growth zones are revealed by cathodoluminescence and birefringence in 78% of the Group A diamonds. Of these, more than half show an initial stage of regular, continuous growth from their point of nucleation (Fig. 6*a*), with thick oscillatory-zoned layers similar to diamonds from cratonic occurrences such as Siberia (Bulanova, 1995). The other 25% show multistage octahedral growth histories with at least two stages of growth, each truncated by resorption events (Fig. 6*d*). Approximately 6% of the diamonds show cubo-octahedral growth centres with octahedral zoning on rims, and two diamonds show sector structures (Fig. 6d). Twenty percent of the Group A diamonds, with high N contents, show homogeneous growth in cathodoluminescence.

In the Group A diamonds with simple octahedral growth morphologies, growth nuclei are commonly off-centre. Two stones, with rounded dodecahedral external morphologies, are fragments of larger structures with a face and corner preserved (Fig. 6*c*). This is evidence of a significant degree of late-stage resorption. Diamonds with multistage growth histories commonly show an early stage represented by a N-rich, homogeneous central structure that is rounded from resorption, and a subsequent stage of oscillatory-zoned octahedral layers, with the outermost layers truncated and rounded by a final resorption event (Fig. 6*b*).

Group A diamonds typically have N-rich centres and N poor rims. One third of the stones show a gradation to N-free rims (i.e. Type II according to the terminology of Kaiser and Bond (1959)). It is possible that Type II rims developed on other stones but were lost during resorption.

Growth characteristics of Group B diamonds

Group B diamonds show more complex growth histories. Group B1 diamonds show dynamic histories of rapid growth, dissolution and strain events, while Group B2 diamonds show mostly homogeneous patterns (Fig. 7*d*). The different growth structures also relate to variations in N content (see below). Growth histories of the Group B1 diamonds are characterized by: (1) non-planar growth facets; (2) evidence of strain; and (3) rare sector growth. Many stones show homogeneous N-rich central structures rounded by resorption. Outer zones show dark cathodoluminescence colours indicating lower N contents with thick concentric Type I and Type II zones with sharp contacts that are also rounded from rapid growth, and in some cases dissolution (Fig. 7*b,d*).

Strain patterns are visible as sub-parallel bands enclosing cross-hatched deformation lines that are blue and yellow in cathodoluminescence. Strain patterns overprint growth structures and show disruption of layers (Fig. 7*b*) and brecciation of structures in more deformed stones (Fig. 7*c*). Where diamond is rehealed, it is Type II. Evidence that deformation coincided with diamond growth occurs where there is regrowth of Type II diamond in deformation displacements and subsequent overgrowths of deformation zones.

Sectorial structures (distinct from sector zoning) also occur in many Group B1 diamonds that have multiple directions of deformation. The sectors have the same orientation as the deformation surfaces indicating that sector zoning in these stones may be a result of deformation (Fig. 7*d*). One Group B1 diamond shows true sector growth. Sectors are visible because of the concentric zoning directions, and the difference in N between adjacent limbs as preferential partitioning of N impurities occurs between cubic and octahedral growth directions, thus indicating cubo-octahedral form (Frank *et al.*, 1990). Because of the large degree of post-growth resorption, cubo-octahedral faces are not preserved in surface morphologies.

Group B2 diamonds have homogeneous internal structures, also with blue cathodoluminescence. A small number of these diamonds show N-poor intergrowths or rim zones that have strained cathodoluminescence patterns similar to those of Group B1. One Group B2 diamond contains strained intergrowths that are crystallographically oriented on octahedral growth planes, indicating an octahedral form. Type II rims occur on two Group B2 diamonds with sharp internal boundaries.

Significance of internal growth structures

Growth structures provide information about the growth environment of a diamond. Internal structures in diamond monocrystals typically show concentric zoning parallel to octahedral (111) planar interfaces. These structures are interpreted to indicate stable conditions of growth that were: (1) slow; (2) in low C supersaturation conditions; and (3) in the presence of a fluid or melt (e.g. Sunagawa, 1984*b*).

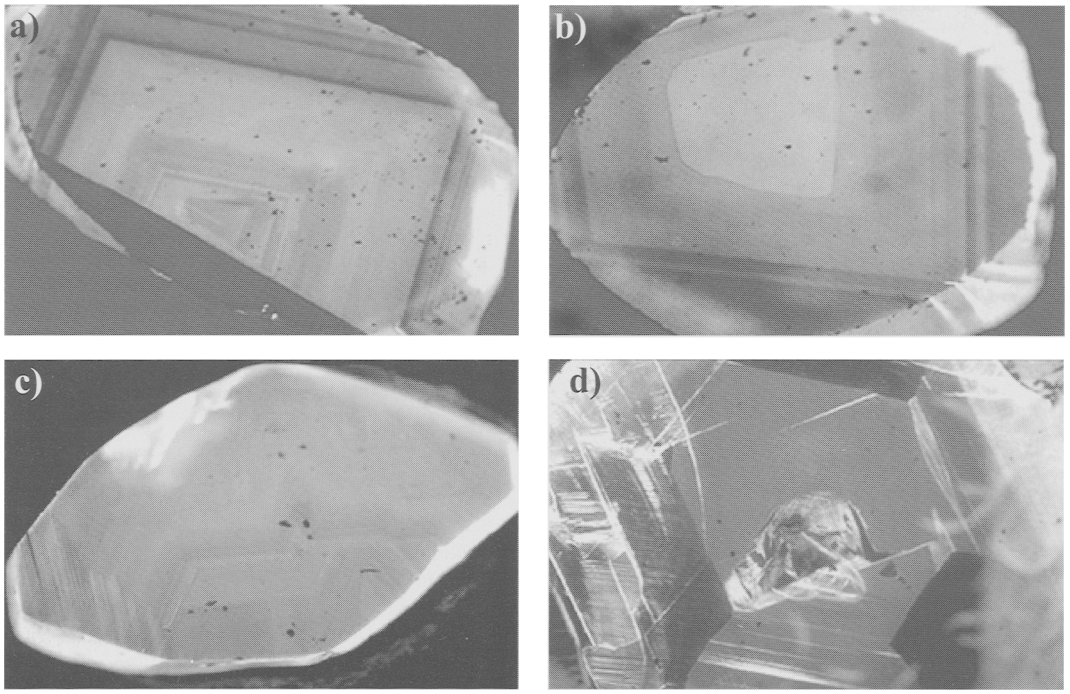

FIG. 6. (*a*) Cathodoluminescence image of a Group A diamond plate showing concentric zoning with octahedral patterns. Shades of grey indicate blue CL colours. Lightest hues indicate highest N contents while dark CL colours indicate very low N contents. (*b*) A Group A diamond plate showing two stages of growth. The central zone (which is homogeneous in structure and contains the highest N content) is rounded from resorption. The central zone is overgrown by concentric octahedral layers of decreasing N content towards the rim. Diamonds are all ~3 mm in diameter. (*c*) A Group A diamond plate with a rounded external morphology consists of a partially preserved octahedral form with only one edge of a larger crystal preserved. (*d*) A Group A diamond with sector growth. The central zone contains a large irregular shaped olivine inclusion. The sectors vary between Type I and Type II diamond (see text), indicative of a cubo-octahedral form.

Concentric oscillatory zoning indicates temporal variation in growth conditions and may indicate changes in environmental factors including pressure and temperature, fluid/melt composition and redox conditions (e.g. Allègre *et al.*, 1981). There is debate as to whether oscillatory zoning patterns reflect internal self organization with impurity distribution controlled by diffusion and fluid interaction with the growing crystal (Allègre *et al.*, 1981; Ortoleva, 1990; Reeder *et al.*, 1990) or conversely environmentally controlled fluctuations from open system growth (Holten *et al.*, 1997). In either case such fluctuations are forced by external changes in conditions (Holten *et al.*, 1997). In the Wellington Group A diamonds, the observation that N content decreases between zones from core to rim suggests that growth rates slowed through time, with more impurities incorporated during early rapid growth (Kamiya and Lang, 1964), or that oxygen fugacity conditions increased during growth (Humbert *et al.*, 1997).

Differences between planar and non-planar facets observed between early and late growth in some Group A diamonds, and Group B diamonds are also important. Non-planar facets observed at the intermediate zones of some Group A diamonds, and the majority of Group B1 diamonds suggest rapid growth rates and conditions less stable than those that favour planar growth faces (O'Hara *et al.*, 1968, Jamtveit and Andersen, 1994).

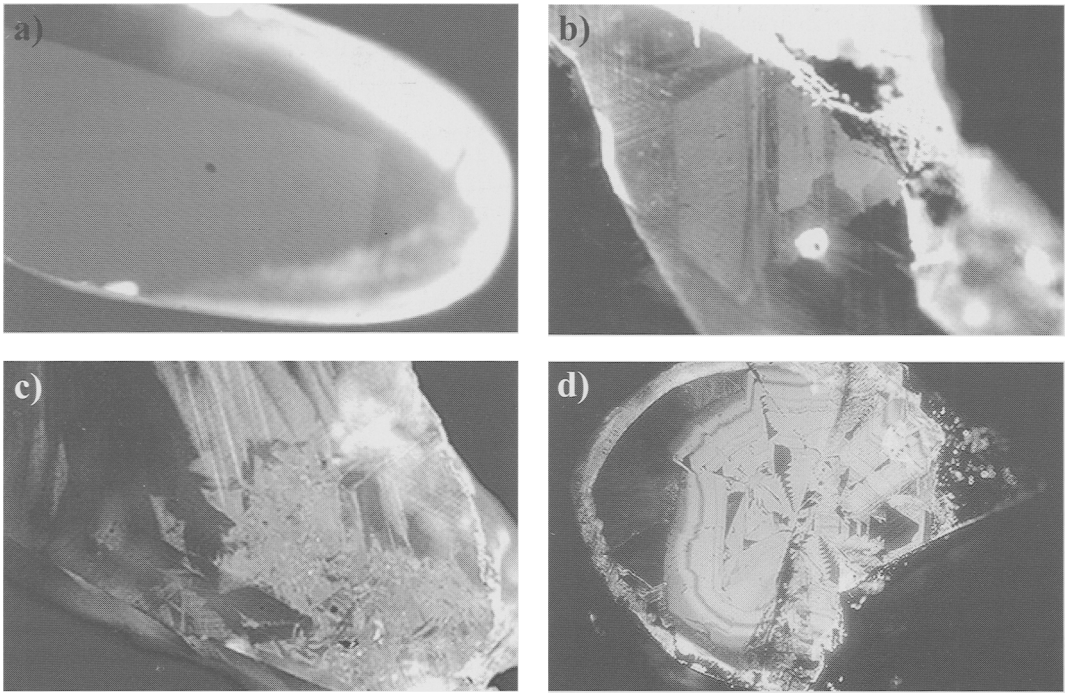

FIG. 7. Cathodoluminescence images of diamond plates: diamonds are all ~3 mm in diameter. (*a*) A Group B2 diamond plate showing an homogeneous central structure with a Type II (N free) overgrowth showing a distinct planar boundary between the growth zones. (*b*) A Group B1 diamond plate with a hexagonal to rounded N rich central structure that shows evidence of displacment of layers as a result of deformation. The displaced area is infilled by Type II diamond. Rims are low in N (dark cathodoluminescence) and show evidence of plastic deformation with fine cross-hatched lamination lines. (*c*) A Group B1 diamond plate with strain patterns. The zone of strongest deformation shows brecciation of structures. (*d*) A Group B1 diamond plate with sector growth structures that in this case are controlled largely by deformation.

Sector growth and cubo-octahedral to octahedral zoning

Sector growth represents compositional differences between adjacent crystallographically non-equivalent sectors, inferred to be due to differential surface impurity adsorption (Northrup and Reeder, 1994). Sector growth in diamond is visible in cathodoluminescence because of the preferential partitioning of N impurities between cubic and octahedral growth directions (Frank *et al.*, 1990).

Two types of sector growth are seen in the Wellington diamonds: (1) sector growth throughout whole stones in which sectors radiate from amorphous seed structures, suggesting cubo-octahedral growth forms (Fig. 6*d*); and, more commonly, (2) cubo-octahedral centres with intercalated cubic and octahedral layers (resulting in what is termed the "centre cross pattern" (Seal, 1965)), that are grown over by octahedral outer layers.

Fibrous cubic growth layers in the centre of a diamond may be an indication of lower temperatures (Harris, 1992) or rapid growth at the time of and following diamond nucleation. Unstable growth conditions may have been caused by the need to overcome the nucleation field strength of diamond (Bulanova, 1995). Tangential growth mechanisms with octahedral form dominate when growth rates have slowed and stabilized (Sunagawa, 1984).

Summary of growth histories of the Wellington diamonds

The majority of diamonds from Wellington (except those with sector growth), show a

decrease in N content from core to grain boundary (Figs 6*a,b*).

Group A

Group A diamonds show internal growth characteristics which suggest that they grew slowly with some fluctuations in mantle conditions. The octahedral form predominates, and ~7% of diamonds show cubic habits at early growth stages, analogous to Yakutian diamonds (Bulanova, 1995). About 25% of Group A diamonds have a history of growth and resorption events indicative of environmental changes during growth, with unstable conditions creating one or more episodes of diamond dissolution. Several diamonds in this category do not show truncation of growth layers, but, instead, a series of non-planar facets, possibly reflecting a period of rapid growth with instability. The final severe resorption stage observed for all Wellington diamonds is inferred to have occurred during transportation to the Earth's surface in a lamproitic-type magma.

Group B

Group B diamonds contain evidence of growth under a stress field. Internal structures in the Group B1 diamonds show centrally resorbed forms with overgrowths of non-planar facets, and rare sector growth. Evidence of strain during growth is observed as deformation lamellae with multiple orientations, disruption of growth layers with infilling of Type II diamond, and internal brecciation structures (Figs 7*b,c,d*). Group B2 diamonds appear to have grown in more stable conditions than Group B1 diamonds, as they show mostly homogeneous growth structures (Fig. 7*a*). Where zoning is observable, sharp primary octahedral growth faces are evident, indicating evidence of growth in stable conditions without resorption. Evidence of deformation is observed on the external faces of Group B2 diamonds with abundant deformation and defect-controlled pitted hemispherical cavities. However these structures are not as strongly developed as in Group B1. Deformation is also evident in the internal parts of stones with low N contents. Abundant N in an aggregated form may mask evidence of strain and deformation in cathodoluminescence, and may inhibit formation of strain features, possibly by strengthening structural bonds (Milledge, pers. comm.)

Nitrogen aggregation states and mantle deformation in the Wellington diamonds

Nitrogen aggregation in Group A diamonds

Nitrogen aggregation in Type I diamond is a process that Allen and Evans (1981) showed experimentally to be dependent on time (t), temperature (T) and pressure. However, Evans (1992) suggested N aggregation may also be dependent on applied stress during growth or mantle storage and thus may not directly reflect temperature-time relationships.

It has been shown that with increasing temperature, single N atoms (termed 1b) will aggregate in the diamond lattice, to form progressively two N atoms on adjacent lattice sites (IaA), then a tetrahedral grouping of N plus a vacancy around a C atom (IaB). The latter corresponds to platelet development (e.g. Evans and Harris, 1989).

Preliminary N content and N aggregation data integrated with growth histories of Group A diamonds show that they fall into two subgroups. The majority of diamonds (Group A1) show a linear correlation between N content (250–2500 at. ppm) and the amount of IaB aggregation (6–42%). This indicates that they may share a similar time-temperature-strain history. A small group of stones (Group A2) has low N contents (140–900 at. ppm) relative to high IaB N aggregation states (44–95%), some with platelet degradation. These stones show evidence of multiple growth stages with complex central structures, fine zoning on grain boundaries and common evidence of deformation (Table 1; Fig. 8)

Nitrogen aggregation in Group B diamonds

Group B1 diamonds have low N contents <400 at. ppm. Group B2 diamonds on the other hand have high N contents; 900 to 3000 at. ppm. Both groups show a higher degree of N aggregation, relative to N contents when compared with most Group A diamonds; the low N Group B1 has <12% IaB, and the high N Group B2 has 33–63% IaB. The proportional relationship between N content and percent IaB indicates that both Group B1 and B2 share similar temperature-time-strain histories (Fig. 8).

We have made mantle storage temperature-time estimates using the spreadsheet program of Mendelssohn *et al.* (1995) and can show that at 1.6 Ga (using the inferred storage time of Taylor

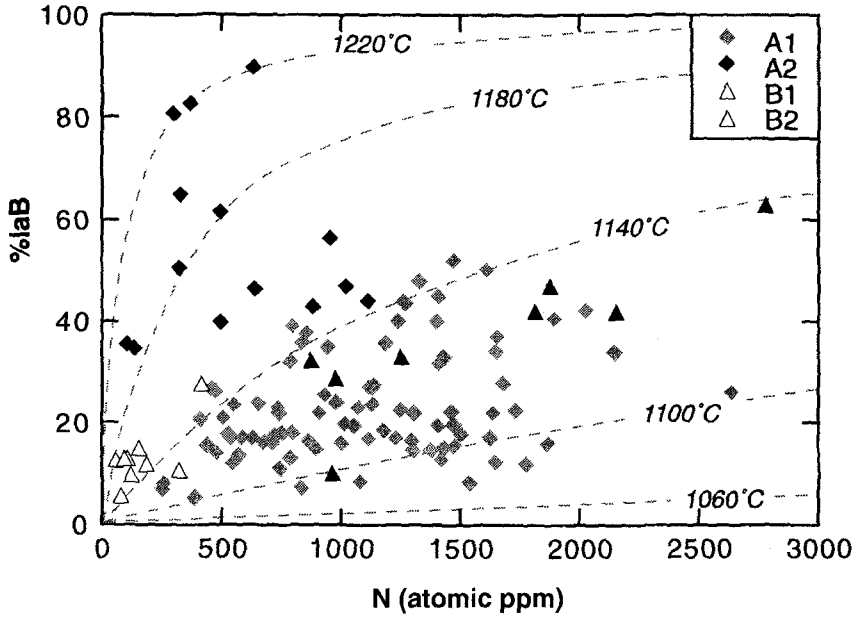

FIG. 8. FTIR data plotted as N contents *vs* N aggregation states for the Group A and Group B Wellington diamonds. Isotherms are plotted for a mantle residence time of 1.6 Ga.

et al., 1990), Group B1 diamonds would have a storage T of ~1160°C, and Group B2 of 1120°C. Group A1 give slightly lower mantle storage temperatures and Group A2 high temperatures (1140–1215°C). There is however, no validated mantle age for these diamonds and thus no appropriate basis for calculating temperatures of mantle storage if this is at all meaningful when there is evidence of strong deformation.

A very significant and relevant problem with these isotherm calculations is that any estimated age between 0.3 and 3 Ga results in temperatures that are only 10s of degrees different and therefore not meaningful. For example, Meyer *et al.* (1997) demonstrated that ages ranging from 0.3 to 3.1 Ga can be derived from the same data, for a narrow range of mantle storage temperatures (1180 to 1240°C). Similarly, use of the isochron plots results in possible ages exceeding the Earth's geological record: e.g. assumption of a reasonable T of 1120°C gives a range of ages from 1.1 to >10 Ga for all Wellington diamonds. Diamonds from the same population group can yield a 2 Ga difference in calculated age. Thus far, the only valuable information evident from these data is that Group B1 has more plastic deformation and also higher storage temperatures than Group B2 (Fig. 8). Group A2 with the low N and high plastic deformation gives the highest storage temperature estimates with a scatter between 1140 and 1215°C at an assumed mantle storage time of 1.6 Ga. This result strongly indicates that deformation may enhance N aggregation states.

Therefore, we suggest that the high degree of N aggregation, particularly in the Group B1 stones, may be due to deformation (Evans *et al.*, 1995) and is not necessarily an indication of long storage in the mantle, as has been suggested by Taylor *et al.* (1990).

Summary of diamond characteristics

Characteristics of the Wellington alluvial diamonds are summarized in Table 1. All of these diamonds have surfaces that are highly resorbed and polished, with most stones showing no evidence of external primary growth faces. Most diamonds appear to have been reduced to about half their normal size by resorption. Two discrete groups of diamonds are recognized:

Group A diamonds (80%)

These have external dodecahedral and tetrahexahedroid forms, growth forms with octahedral

zoning, common radiation damage, abrasion structures, dominance of inclusions of the peridotitic paragenesis, $\delta^{13}C$ between −10 and −3‰, generally high N contents (250–2500 at. ppm), decreasing N content from core to rim, N aggregation states ranging between 10 and 95% IaB, and a correlation between growth structures, N contents and N aggregation states.

Group B diamonds (20%)

These commonly have irregular flat or elongate dodecahedral forms preserving micro-ring pits on polished low relief faces of very resorbed surfaces, heavy abrasion (relative to Group A), rare radiation damage, inclusions of a Ca-rich variety of the eclogitic paragenesis (diopside, omphacite, coesite and garnet), and relatively heavy C isotopic ratios ($\delta^{13}C$ −5‰ to +3‰). Large pitted hemispherical cavities indicate abundant dislocation defects. Deformation features indicate deformation during growth and mantle storage. Group B1 diamonds have low N contents (<400 at. ppm) and show rounded growth layers that suggest unstable growth with rare sector growth, and strongly strained internal growth patterns. Group B2 diamonds have high N contents (>900 at. ppm) and homogeneous internal structures. Nitrogen aggregation states average ~12% IaB for Group B1 and 35% IaB for Group B2. The percentage of IaB aggregation relative to N content is higher for Group B than for Group A.

Discussion

Origin of the Wellington Group A diamonds

The dominant inclusion suite of the Group A diamonds identified in this study is similar to that for peridotitic diamonds from kimberlites and lamproites worldwide (Meyer, 1987), except that orthopyroxene and garnet have not been observed. Major element compositions of the eclogitic mineral inclusions lie within the worldwide data range. The presence of wüstite as central inclusions suggests nucleation under reducing conditions. $\delta^{13}C$ values are similar to world averages for eclogitic and peridotitic diamonds.

Fluctuating conditions during the intermediate growth stages are indicated by resorption and oscillatory zoning patterns. In the later stages of growth, diamonds show a gradation to lower N contents that may correspond to increasing f_{O_2} conditions (Humbert *et al.*, 1997), or a decrease in growth rate with decreased impurity absorption (Cartigny *et al.*, 1997). The common multiple growth stages and the strong resorption of both the N rich intermediate zones and the overgrowths of oscillatory-zoned low-N rims, indicate periods of instability such as changes in pressure, temperature, oxygen fugacity and/or composition of the surrounding medium. About half of the Group A diamonds show clear evidence of deformation indicating that the diamonds were stored, and may have grown in subsolidus conditions. The two sub-groups of Group A diamonds based on N aggregation states and N content may indicate two distinct time-temperature histories for the two sub-groups, or may simply reflect variations in deformation history within a single population. The common green and brown radiation spots and evidence of abrasion structures indicate long and varied residence in alluvial environments.

The Group A diamonds are generally similar in their primary crystal forms, internal growth structures, mineral inclusion compositions and C isotope compositions to those found with kimberlitic/lamproitic hosts in Archaean and Proterozoic cratons. This, along with the nature of the surface abrasion structures and radiation damage, suggests that the Group A diamonds may represent an older population of peridotitic diamonds that have been in secondary collectors longer than the Group B.

If this is so, the age and location of the host rocks is still unidentified. There is sparse geological evidence for Proterozoic lithospheric components in eastern Australia (and none for Archaean). Some of the tectonic models for the Lachlan Fold Belt (e.g. Collins and Vernon, 1994) call for rifting and delamination of Archaean and Proterozoic lithosphere that accreted through the Phanerozoic. Handler *et al.* (1997) recorded Proterozoic Re-Os isotopic model ages for lithospheric mantle components beneath Mt Gambier (eastern South Australia) and western Victoria. Zhang and O'Reilly (1997) have recorded Proterozoic model ages for mantle source regions of basalts beneath Central NSW. At this stage we cannot identify a source region or specific time of transportation to the surface for these Group A diamonds. However, Veevers (1994) has traced Lower Permian fluvio-glacial drainage patterns from east Antartica to south eastern Australia and shown (Veevers, pers. comm.) that the distribution of *c.* 600 Ma zircons in eastern Australian

sediments is consistent with their provenance from Antartica. Therefore Precambian Antarctic terrains are a possible source for the Group A diamonds.

Origin of the Group B diamonds

Group B diamonds crystallized principally in an eclogitic environment as evidenced by inclusions. $\delta^{13}C$ values are heavy (most range between -0.9 to 2.9‰ with one at -5‰). This may be due to the contribution of marine carbonates in the source (Kirkley *et al.*, 1991) or isotopic enrichment through precipitating graphite or diamond by decarbonation reactions at low temperatures (300–500°C; Hoefs, 1980; Griffin *et al.*, 1998). These geochemical data are consistent with the formation of the Group B diamonds from a basaltic protolith such as altered ('rodingitized') ocean-floor basaltic rocks in a subducting slab (Griffin *et al.*, 1998).

The Group B diamonds show unambiguous evidence of strong deformation during growth including displaced and brecciated zones and deformation lamellae truncated by subsequent growth layers in the low N diamonds. The homogeneous growth structures of the high-N Group B diamonds may reflect masking of deformation structures or resistance to deformation because of the high concentrations of N bonded in an aggregated state (Milledge, pers. comm.). Deformation features in Group B diamonds indicate a high strain environment consistent with that in a subducting slab. The high degree of N aggregation may be a result of deformation (Evans, *et al.*, 1995) and is not necessarily an indicator of long mantle residence as proposed by Taylor *et al.* (1990).

Group B stones show rare evidence of radiation damage although both brown and green spots occur, suggesting (like Group A) a significant time in an alluvial system.

$^{39}Ar/^{40}Ar$ emplacement ages of clinopyroxene inclusions recorded by Burgess *et al.* (1998) for the diamonds of the Group B type from Copeton, are Carboniferous to Mid- Permian (340 ± 28 Ma). Burgess *et al.* (1998) favour a cratonic origin for these diamonds followed by transport in Permian glaciers, but the ages could also be interpreted in support of a young subduction origin (see Griffin *et al.*, 1998). A young age would uniquely distinguish the diamonds from cratonic ones and link them to the tectonic development of the Tasman orogen.

Surface emplacement of Group A and B diamonds at Wellington

Both Group A and Group B diamonds show etch structures comparable to those of diamonds from kimberlites and lamproite occurrences (e.g. McCallum *et al.*, 1994) and severe resorption, proving transport to the Earth's surface by magma. Furthermore, the very lustrous nature of the surface polish suggests that the diamonds were transported to the surface in a magma more like a lamproite than a kimberlite (Hall and Smith, 1985). The similarity in surface characteristics suggests that Groups A and B had a similar style of emplacement, although sampled from a different sources and probably at different times.

No kimberlitic or lamproitic pipes are known in eastern Australia although they may have been obscured by subsequent erosion and sedimentation. The location of Tertiary basalt flows in eastern Australia coincides with diamond distribution (diamonds are commonly concentrated in underlying deep leads), but there is no evidence to suggest that the basalts are a source of diamond (see Griffin *et al.*, 1998). The association of basalts and diamonds reflects the fact that most of the Tertiary basalts flowed down river valleys, covering river gravels containing diamonds.

If the Wellington diamonds are derived from the mantle in eastern Australia, they were removed from the mantle prior to 200 Ma when high geotherms from basaltic volcanic activity become characteristic of eastern Australian terranes – conditions under which diamonds would not survive (e.g. O'Reilly and Griffin, 1985; O'Reilly, 1989).

The absence of resistate diamond indicator minerals, the considerable mechanical abrasion, evidence of a history of exposure to U or Th radiation for Group A stones (presumably during surface residence) and sorting of diamond size, shape and quality (so that only rounded stones averaging ~ 0.2 carats are found near Wellington), all indicate a long residence time at the earths surface. Each Group, A and B, was sampled from a different primary source region and probably at different times. The Wellington diamond suite is a mixture of both populations. The two Wellington diamond groups are recognized as nearly pure concentrations at other alluvial deposits, 160 km south east at Airly Mountain (Group A) and 350 km north east at Bingara (Group B), New South Wales.

Conclusions

On the basis of a study of more than 500 diamonds from Wellington, NSW, diamonds fall into two distinct groups with significantly different petrogenesis. Group A diamonds are similar to diamonds brought to the surface by kimberlites or lamproites world-wide. Their characteristics including internal structures and inclusions indicate growth in the presence of fluid activity under fluctuating conditions in the mantle, possibly in Proterozoic-type depleted peridotitic lithosphere. Group B diamonds on the other hand formed in a high strain environment. They are distinct from other diamonds in the combination of their surface features, internal structures, heavy C isotopic compositions, and the dominant eclogite/calc-silicate paragenesis of the inclusions. These features are consistent with their formation on a subducted slab during Late Palaeozoic (Carboniferous or possibly Permian) subduction, and subsequent magmatic transportation to the surface. Transport would need to have followed subduction cessation by not more than 30 Ma so that the diamond could not re-equilibrate to graphite as the slab warmed (Griffin *et al.*, 1998).

Acknowledgements

We thank Rio Tinto (formerly CRAE) for funding RMD's stipend and research support for three years. Jacob Rebek and Chris Smith assisted in the shaping of this project and Chris Smith provide valuable assistance in understanding diamond morphology, and has provided comments throughout the project. Luc Daigle, while at CRAE, organized the availability of the Wellington diamonds and Col Ribeaux, those from Airly Mountain. Galina Bulanova is thanked for discussions about growth structures; Judith Milledge supervised RMD for three months at University College London, providing unique insights into diamond studies and shared her expertise in FTIR; and Jeff Harris unstintingly shared his knowledge of all aspects of diamonds. Anita Andrew developed the C isotope method of analysis at CSIRO and her expertise, assistance and advice, along with that of Andrew Todd, were invaluable. Argyle Diamonds' polishing and laser cutting facilities, in particular Leo Smans, Damon Sweeny and Martin Volk, were generous with time, advice and equipment. Norm Pearson and Carol Lawson provided expertise and assistance with the electron microprobe; Tony Vassalo's advice and generous access to the FTIR facility at CSIRO, North Ryde is much appreciated. Allan Giles' assistance with the cathodoluminescence facility at UTS is gratefully acknowledged. The final version of this manuscript has been significantly improved and clarified by the detailed and constructive comments of Jeff Harris and anonymous reviewers.

This is publication number 110 from the ARC National Key Centre for the Geochemical Evolution and Metallogeny of Continents (GEMOC).

References

Allan, A.D. and Leitch, E.C. (1990) The nature and origin of eclogite blocks in serpentinite from the Tamworth Belt, New England Fold Belt, eastern Australia. *Austral. J. Earth Sci.*, **37**, 43–9.

Allen, B.P. and Evans, T. (1981) Aggregation of nitrogen in diamond, including platelet formation. *Proc. Roy. Soc. Lond.*, **A375**, 93–104.

Allègre, C.J., Provost, A. and Jaupart, C. (1981) Oscillatory zoning: a pathological case of crystal growth. *Nature*, **294**, 223–8.

Bai, W.J., Zhou, M.F. and Robinson, P. T. (1993) Possibly diamond-bearing peridotites and podiform chromites in the Luobusa and Donqiao ophiolites, Tibet. *Canad. J. Earth Sci.*, **30**, 1650–9.

Barron, L.M., Lishmund, S.R., Oakes, G.M. and Barron, B.J. (1994) Subduction diamonds in New South Wales: Implications for exploration in eastern Australia. *Q. Notes, Geol. Surv. New South Wales*, **94**, 1–23.

Barron, L.M., Lishmund, S.R., Oakes, G.M., Barron, B.J. and Sutherland, F.L. (1996) Subduction model for the origin of some diamonds in the Phanerozoic of eastern New South Wales. *Austral. J. Earth Sci.*, **43**, 257–67.

Brown, R.E. (1995) Mineral deposits of the Bingara, Croppa Creek, Gravesend and Yallaroi 1:100 000 sheet areas. *Q. Notes, Geol. Surv. New South Wales*, **98**, 1–32.

Bulanova, G.P. (1995) The formation of diamond. *J. Geochem. Expl.*, **53**, 1–23.

Bulanova, G.P., Griffin, W.L., Ryan, C.G., Shestakova, O.Y. and Barnes, S.-J. (1996) Trace elements in sulfide inclusions from Yakutian diamonds. *Contrib. Mineral. Petrol.*, **124**, 111–25.

Bulanova, G.P., Griffin, W.L. and Ryan, C. G. (1998) Nucleation environment of diamonds from Yakutian kimberlites, *Mineral. Mag.*, **62**, 409–19.

Burgess, R., Phillips, D., Harris, J.W. and Robinson, D.N. (1998) Diamonds in South-eastern Australia?

Hints from $^{40}Ar/^{39}Ar$ Laser Probe Dating of Clinopyroxene Inclusions from Copeton Diamonds. *Ext. Abst. 7th Int. Kimberlite Conf., Cape Town*, pp. 119–21.

Cartigny, P., Boyd, S.R., Harris, J.W. and Javoy, M. (1997) Nitrogen isotopes in peridotitic diamonds from Fuxian, China: the mantle signature. *Terra Nova*, **9**, 175–9.

Collins, W.J. and Vernon, R.H. (1992) Palaeozoic arc growth, deformation and migration across the Lachlan Fold Belt, southeastern Australia. *Tectonophys.*, **214**, 381–400.

Collins, W.J. and Vernon, R.H. (1994) A rift-drift-delamination model of continental evolution: Paleozoic tectonic development of eastern Australia. *Tectonophys.*, **235**, 249–75.

Dobrzhinetskaya, L.F., Eide, E.A., Larsen, R.B., Sturt, B.A., Tronnes, R.G., Smith, D.C., Taylor, W.R. and Posukhova, T.V. (1995) Microdiamond in high-grade metamorphic rocks of the Western Gneiss region, Norway. *Geology*, **23**, 597–600.

Evans, T. (1992) Aggregation of nitrogen in diamonds. In *The Properties of Synthetic and Natural Diamonds* (J.E. Field, ed.), pp. 259–90, Academic Press.

Evans, T. and Harris, J.W. (1989) Nitrogen aggregation, inclusion equilibration temperatures and the age of diamonds. In *Kimberlites and Related Rocks, Vol. 2, Their Mantle/Crust setting* (J. Ross, ed.), *Geol. Soc. Aust. Special Publ.*, **14**, 1002–6.

Frank, F.C., Lang, A.R., Evans, D.J.F., Rooney, M.L.T., Spear, P.M. and Welbourn, C.M. (1990) Orientation-dependent nitrogen incorporation of vicinals on synthetic diamond cube growth surfaces. *J. Cryst. Growth*, **100**, 354–76.

Griffin, W.L., O'Reilly, S.Y. and Davies, R.M. (1998) Subduction-related diamond deposits? Constraints and possibilities. *Rev. Econ. Geol*, in press.

Hall, A.E. and Smith, C.B. (1985) Lamproite diamonds – are they different? In *Kimberlite Occurrence and Origin: A basis for conceptual models in exploration* (J.E. Glover and P.G. Harris, eds). The University of Western Australia, Publ. No. **8**, pp. 167–212.

Handler, M.R., Bennet, V.C. and Esat, T.M. (1997) The persistence of off-cratonic lithospheric mantle: Os isotopic systematics of variably metasomatised southeast Australian xenoliths. *Earth Planet. Sci. Lett.*, **151**, 61–75.

Harris, J.W. (1992) Diamond Geology. In *The Properties of Synthetic and Natural Diamonds*, (J. E. Field, ed.). Academic Press, pp. 325–93.

Hoefs, J. (1980) *Stable Isotope Geochemistry*. Springer-Verlag, Berlin, pp. 208.

Holten, T., Jamtveit, B., Meakin, P. Cortini, M., Blundy, J. and Austrheim, H. (1997) Statistical characteristics and origin of oscillatory zoning in crystals. *Amer. Mineral.*, **82**, 596–606.

Humbert, F., Libourel, G., Marty, B. and France-Lanord, C. (1997) Nitrogen solubility in silicate melt under oxidized and reduced conditions using laser extraction/static mass spectrometry analysis. *Abstr. 7th Ann. V.M. Goldschmidt Conf.*, pp. 101–2.

Joris, A. (1983) Some uncuttable diamonds from N.S.W., Australia, *Indiaqua*. **36**, 41–3.

Jamtveit, B. and Andersen, T.B. (1994) Morphological instabilities during rapid growth of metamorphic garnets. *Phys. Chem. Min.*, **19**, 176–84.

Kaiser, W. and Bond, W.L. (1959) Nitrogen, a major impurity in common Type I diamond. *Phys. Rev.*, **115**, 857–63.

Kamiya, Y., and Lang, A.R. (1964) On the structure of coated diamonds. *Phil. Mag.*, **11**, B347–56.

Kirkley, M.B., Gurney, J.J., Otter, M.L., Hill, S.J. and Daniels, L.R. (1991) The application of C isotope measurements to the identification of the sources of C in diamonds: a review. *Appl. Geochem.*, **6**, 477–94.

Lang, A.R. (1964) Dislocations and the origin of trigons. *Proc. Roy. Soc. Lond.*, **A278**, 234–42.

MacNevin, A.A. (1977) *Diamonds in New South Wales*. Mineral Resources No. **32**, Department of Mines, Geological Survey of New South Wales, 125 p.

Mahlzahn, H. (1997) Diamonds. In *Gem News, Gems and Gemology (Spring edition)*, pp. 60–1.

McCallum, M.E., Huntley, P.M., Falk, R.W. and Otter, M.L. (1994) Morphological, resorption and etch feature trends of the diamonds from kimberlite populations within the Colarado-Wyoming Stateline District, USA. In *Diamonds: Characterisation, Genesis and Exploration, Vol. 2* (H.O.A. Meyer and O.H. Leonardos, eds). CPRM Spec. Publ. **1B**, Brasilia, pp. 32–50.

Mendelssohn, M.J. and Milledge, H.J. (1995) Geologically significant information from routine analysis of the mid-infrared spectra of diamonds. *Int. Geol. Rev.*, **37**, 95–110.

Mendelssohn, M.J., Milledge, H.J., Vance, E.R., Nave, E. and Woods, P.A. (1983) Internal radioactive haloes in diamond. In *Diamond Research*. London, Industrial Diamond Information Bureau, pp. 31–6.

Meyer, H.O.A. (1987) Inclusions in Diamond. In *Mantle Xenoliths* (P.H. Nixon, ed.). John Wiley & Sons, New York and Chichester, pp. 501–22.

Meyer, H.O.A., Milledge, H.J. and Sutherland, F.L. (1995) Unusual diamonds and unique inclusions from New South Wales, Australia. *Abst., 6th Int. Kimberlite Conf., Novosibirsk, Russia, pp. 379–81.*

Meyer, H.O.A., Milledge, H.J. and Temby. P. (1997) Unusual diamonds and unique inclusions from New South Wales, Australia, *Russ. Geol. Geophy.*, **38**, 305–31.

Northrup, P.A. and Reeder, R.J. (1994) Evidence for the

importance of growth-surface structure to trace element incorporation in topaz. *Amer. Mineral.*, **79**, 1167–75.

O'Hara, S., Tarshis, L.A., Tiller, W.A. and Hunt, J.P. (1968) Discussion of interface stability of large facets on solution grown crystals. *J. Cryst. Growth*, **3–4**, 555–61.

O'Reilly, S.Y. (1989) Nature of the east-Australian lithosphere. In *Intraplate Volcanism in Eastern Australia and New Zealand*, (R.W. Johnson ed.). Cambridge University Press, pp. 290–7.

O'Reilly, S.Y. and Griffin, W.L. (1985) A xenolith-derived geotherm for southeastern Australia and its geophysical implications. *Tectonophys.*, **111**, 41–63.

O'Reilly, S.Y. and Griffin, W.L. (1995) Trace element partitioning between garnet and clinopyroxene in mantle-derived pyroxenites and eclogites: P-T-X controls. *Chem. Geol.*, **121**, 105–30.

Orlov, Y. L. (1977). *The Mineralogy of the Diamond.* John Wiley & Sons, New York, 342 p.

Ortoleva, P.J. (1990) Role of attachment kinetic feedback in the oscillatory zoning of crystals grown from melts. *Earth Sci. Rev.*, **29**, 3–8.

Pearson, D.G., Davies, G.R. and Nixon, P.H. (1993) Geochemical constraints on the petrogenesis of diamond facies pyroxenites from the Beni Bousera peridotite massif, North Morocco. *J. Petrol.*, **34**, 125–72.

Pearson, D.G., Davies, G.R. and Nixon, P.H. (1995) Orogenic ultramafic rocks of ultrahigh-pressure (diamond facies) origin. In *Ultrahigh Pressure Metamorphism* (R.G. Coleman and X. Wang, eds). Cambridge University Press, pp. 456–510.

Pouchou, J.L. and Pichoir, F. (1984) A new model for quantitative X-ray microanalysis. Part 1: application to the analysis of homogeneous samples. *Recherche Aérospatiale,* **5**, 13–38.

Reeder, R.J., Fagioli, R.O. and Meyers, W.J. (1990) Oscillatory zoning of Mn in solution-grown calcite crystals. *Earth Science Rev.*, **29**, 39–46.

Roberts, J. and Engel, B.A. (1987) Depositional and tectonic history of the southern New England Orogen, *Aust. J. Earth. Sci.*, **34**, 1–20.

Robinson, D.N. (1980) *Surface textures and other features of diamonds*. Ph.D. thesis (unpublished), University of Cape Town, Rondebosch, South Africa, 221 p.

Robinson, D.N., Scott, J.A., van Niekerk, A. and Anderson, V.G. (1989) The sequence of events reflected in the diamonds of some southern African kimberlites. In: *Kimberlites and Related Rocks, Vol. 2, Their Mantle/Crust setting* (J. Ross, ed.). Geol. Soc. Aust. Special Publ., **14**, 990–1000.

Seal, M. (1965) Structure in diamonds as revealed by etching. *Amer. Mineral.*, **50**, 105–25.

Sobolev, N.V. (1985) Crystalline inclusions in diamonds from New South Wales, Australia. In: *Kimberlite Occurrence and Origin: A basis for conceptual models in exploration* (J.E. Glover and P.G. Harris, eds). The University of Western Australia, Publ. No. 8, pp. 213–26.

Sobolev, N.V. and Shatsky, V.S. (1990) Diamond inclusions in garnets from metamorphic rocks: a new environment of diamond formation. *Nature*, **243**, 742–6.

Sobolev, N.V., Yefimova, E.S., Lavrent'yev, Y.G. and Sobolev, V.S.D. (1984) Dominant calcsilicate association of crystalline inclusions in placer diamonds from southeastern Australia. *Dokl. Akad. Nauk. SSSR*, **274**, 172–5.

Sunagawa, I. (1984) Growth of crystals in nature, In: *Materials of the Earth's Interior* (I. Sunagawa, ed.). Terra Scientific Publ. Co. (TERRAPUB), Tokyo, pp. 63–105.

Sunagawa, I., Horita, S. and Sawata, H. (1983) Surface micro-topography of diamonds from Thailand. *J. Gemmol. Soc. Japan*, **10**, 3–35.

Sunagawa, I., Tsukamoto, K. and Yasuda, T. (1984) Surface microtopographic and X-ray topographic study of octahedral crystals of natural diamond from Siberia. In: *Materials of the Earth's Interior* (I. Sunagawa, ed.). Terra Scientific Publ. Co. (TERRAPUB), Tokyo, pp. 331–49.

Sutherland, F.L., Temby, P., Raynor, L.R. and Hollis, J.D. (1994) A review of the East Australian diamond province. In: *Diamonds: Characterisation, Genesis and Exploration, Vol. 2* (H.O.A. Meyer and O.H. Leonardos, eds). CPRM Spec. Publ. **1B**, Brasilia, pp. 170–84.

Taylor, W.R., Jaques, A.L. and Ridd, M. (1990) Nitrogen-defect aggregation characteristics of some Australasian diamonds: Time-temperature constraints on the source regions of pipe and alluvial diamonds. *Amer. Mineral.*, **75**, 1290–310.

Van Heerden, L.A., Gurney, J.J. and Deines, P. (1995) The carbon isotopic composition of harzburgitic, lherzolitic, websteritic and eclogitic paragenesis diamonds from southern Africa: a comparison of genetic models. *S. African J. Geol.*, **98**, 119–25.

Vance, E.R. and Milledge, H.J. (1972) Natural and laboratory alpha-particle irradiation of diamond, *Mineral. Mag.*, **38**, 871–81.

Vance, E.R., Harris, J.W. and Milledge, H.J. (1973) Possible origins of α-damage in diamonds from kimberlitie and alluvial sources. *Mineral. Mag.*, **39**, 349–60.

Veevers, J.J. (1994) Case for the Gamburtsev subglacial mountains of east Antartica originating by mid-Carboniferous shortening of an intracratonic basin. *Geology*, **22**, 593–596.

Xu S., Okay, A.I., Ji, S., Sengor, A.M.C., Su, W., Liu, Y. and Jian, L. (1992) Diamond from the Dabie Shan

metamorphic rocks and its implication for tectonic setting, *Science,* **256**, 80–2.

Zhang, M. and O'Reilly, S.Y. (1997) Multiple sources for basaltic rocks from Dubbo, eastern Australia: geochemical evidence for plume–lithospheric mantle interaction. *Chem. Geol.*, **136**, 33–64.

[*Manuscript received 23 February 1998: revised 16 October 1998*]